Pressure-calcium relationships in perfused mouse hearts

Guy A. MacGowan, Jonathan A. Kirk, Caroline Evans and Sanjeev G. Shroff

AJP - Heart 290:2614-2624, 2006. First published Jan 13, 2006; doi:10.1152/ajpheart.00979.2005

Am J Physiol Heart Circ Physiol 290: H2614–H2624, 2006.
First published January 13, 2006; doi:10.1152/ajpheart.00979.2005.

Pressure-calcium relationships in perfused mouse hearts

Guy A. MacGowan,[1,3,4] Jonathan A. Kirk,[2] Caroline Evans,[2] and Sanjeev G. Shroff[2]

[1]*Cardiovascular Institute and* [2]*Department of Bioengineering, University of Pittsburgh, Pittsburgh, Pennsylvania;* [3]*Department of Cardiology at Freeman Hospital and* [4]*University of Newcastle upon Tyne, Newcastle upon Tyne, United Kingdom*

Submitted 13 September 2005; accepted in final form 10 January 2006

MacGowan, Guy A., Jonathan A. Kirk, Caroline Evans, and Sanjeev G. Shroff. Pressure-calcium relationships in perfused mouse hearts. *Am J Physiol Heart Circ Physiol* 290: H2614–H2624, 2006. First published January 13, 2006; doi:10.1152/ajpheart.00979.2005.—We explored the relationship between left ventricular (LV) pressure and intracellular free calcium concentration ($[Ca]_i$) in the isolated perfused mouse heart. $[Ca]_i$ (rhod-2) and LV pressure were recorded simultaneously. In response to increases in LV volume (Frank-Starling, FS, protocol), there were increases in developed pressure (up to 250%), with no changes in pressure morphology (rise or relaxation time) or $[Ca]_i$ (magnitude and morphology) for up to 10 min. During transient increases in the stimulus interval at a fixed LV volume (mechanical restitution, MR, protocol), developed pressure increased significantly (31.3 ± 1.2%), with relatively small changes in peak systolic $[Ca]_i$ (7.4 ± 1.4%). The relaxation of $[Ca]_i$, however, was prolonged (30.0 ± 5.5%), resulting in prolonged pressure relaxation (21.2 ± 1.9%) and increased area under the calcium transient that paralleled the increase in developed pressure (1:1 ratio). A model-based analysis showed that changes in LV pressure during the MR protocol could be completely explained by altered $[Ca]_i$; it was not necessary to invoke any changes in model parameters (i.e., dynamic processes that link calcium to pressure). For the FS data, the model predicted only a change in the gain parameter; however, this change alone cannot reproduce well-established length-dependent changes in the steady-state force-pCa relationship. In summary, the mouse myocardium appears to be unique in that significant changes in peak developed pressure can occur with little or no change in the peak $[Ca]_i$. Additionally, unlike other mammalian species, load-dependent prolongation of pressure relaxation is absent in the mouse heart, and pressure relaxation is primarily governed by intracellular free calcium relaxation.

murine heart; length-dependent activation; load-dependent relaxation; excitation-contraction coupling; model-based analysis

THE MOUSE HEART has several distinguishing features compared with larger mammals, including an in vivo heart rate of ~600 beats/min (16). Consequently, calcium handling in the mouse myocardium is also different from mammals with longer cardiac cycles. There exists an almost complete dependence on the sarcoplasmic reticulum to provide the calcium for myocyte contraction (4, 18). Gao et al. (12) have characterized calcium cycling and contractile activation in the mouse myocardium. They described a positive force-frequency relationship in isolated mouse myocardium, though the increase in force was greater than that expected from the underlying increase in intracellular free calcium, suggesting "frequency-dependent sensitization" of the myofilaments. Their findings also showed that mouse myofilament had decreased calcium sensitivity and increased cooperativity under steady-state activation relative to other species.

Length-dependent activation in the mouse may have unique features as well. Typically, there are two components of length-dependent activation that are distinguishable from their temporal patterns of responses (1, 2). The fast-acting early component is due to increased calcium sensitivity of the myofilament and is the basis for the Frank-Starling relationship. The slow-acting late component is due to an increase in the calcium transient. Reyes et al. (23) have studied in vivo hemodynamics in the anesthetized mouse by using a conductance catheter to obtain pressure-volume loops. They demonstrated that increasing end-diastolic volume by aortic constriction resulted in an immediate increase in contractility. However, there was no further augmentation in contractility up to 7 min after the increase in load, suggesting that the late component of length-dependent activation was not operative in the mouse. Calcium transients were not measured in this study, and therefore, the potential role of intracellular free calcium in the absence of the late component remains speculative.

The purpose of the current study was to characterize the relationship between pressure and intracellular free calcium in the perfused mouse heart. Specifically, we were interested in the following questions: *1*) Can peak developed pressure change significantly with a minimal change in the peak systolic intracellular free calcium? *2*) Is the late component of length-dependent activation absent? *3*) What are the determinants of pressure relaxation? Two perturbations were used to alter pressure: changes in ventricular volume at a fixed stimulation interval (Frank-Starling protocol) and single-beat changes in stimulation interval at a fixed ventricular volume (mechanical restitution protocol). We used the isolated perfused mouse heart preparation and the calcium-sensitive fluorescent dye rhod-2 to record pairs of left ventricular (LV) pressure and intracellular free calcium concentration ($[Ca]_i$). This allowed us a more physiological assessment of murine myocardium compared with isolated tissue studies, as well as measurements of $[Ca]_i$ that are not possible with in vivo studies.

METHODS

Isolated perfused hearts. This study was approved by the Institutional Animal Care and Use Committee of the University of Pittsburgh and conforms to the *Guide for the Care and Use of Laboratory Animals* published by the National Institutes of Health (NIH Publication No. 85-23, Revised 1996). Male FVB mice of similar age (19.9 ± 1.5 wk) and body mass (36 ± 1.9 g) were anesthetized with an intraperitoneal injection of 2,2,2-tribromoethanol (Avertin, 250 mg/kg

Address for reprint requests and other correspondence: S. G. Shroff, Dept. of Bioengineering, Univ. of Pittsburgh, 749 Benedum Hall, Pittsburgh, PA 15261 (e-mail: sshroff@pitt.edu).

The costs of publication of this article were defrayed in part by the payment of page charges. The article must therefore be hereby marked "*advertisement*" in accordance with 18 U.S.C. Section 1734 solely to indicate this fact.

body wt). Animals were then anticoagulated using 100 units of heparin. Once the heart was excised from the animal, the aorta was quickly cannulated. We then began retrograde aortic perfusion at a constant pressure of 70–80 mmHg. Tissue culture medium (Media 199, Invitrogen, Carlsbad, CA) was used as the perfusate ($CaCl_2$ 1.8 mM). To this solution the following were added: 5.0 mM creatine, 4.8 mM taurine, 6.0 mM carnitine, 2.5 mM sodium pyruvate, 8 μM insulin, and 5.0 μM metoprolol (to eliminate pacing-induced catecholamine release). The solution was oxygenated with 95% O_2-5% CO_2, pH was adjusted to 7.4, and temperature was maintained at 37°C. A balloon made from high-density polyethylene (HDPE, from a plastic shopping bag) was placed in the left ventricle through the mitral valve and secured with a suture though the LV apex. A catheter-tip pressure transducer (MPC-500, Millar Instruments, Houston, TX) was used to measure LV pressure. The balloon volume was altered using a thumb-screw controlled 100-μl microsyringe (Hamilton Gas Tight, Reno, NV). Platinum pacing electrodes were placed on the heart, which was then paced with an interbeat interval of 240 ms using a Pace-1A cardiac stimulator (Radionics, Burlington, MA). Pressure data were digitized online at 500 Hz for later offline analysis.

Fluorescence measurements. Methods to measure intracellular free calcium from the perfused mouse heart using the calcium-sensitive fluorescent dye rhod-2 have previously been described in detail (10, 19). In this study, several equipment modifications from the original descriptions have been made, which include use of a spectrofluorometer equipped with a 150-watt light source and two photomultiplier units (Photon Technology International, Lawrenceville, NJ). The heart was situated in a water-jacketed chamber kept at 37°C and placed against the optical window. Heart motion was prevented by an anterior-to-posterior stabilizer as well as two lateral stabilizers. Three light guides (3 mm core) were coupled to the surface of the mouse heart by placing them within 1 mm of a glass window of the heart warming chamber: one for excitation light, one to collect fluorescence emission, and one to collect reflected light that was used in the calibration of the fluorescence signal. The excitation and fluorescence emission light guides were placed in a horizontal plane and at 30° and 70°, respectively, with respect to the plane of the glass window. The light guide for reflected light was placed 45° above the horizontal plane and at 70° with respect to the glass window.

After baseline measurements, 100 μg of rhod-2 was loaded through the coronary perfusate, and after 20 min, fluorescence and absorbance measurements were taken. Fluorescence time-based scans were performed with excitation at 524 nm and emission at 589 nm, and a long-pass filter (550 nm) placed in the emission light pathway. Fluorescence data were digitized online at 500 Hz for later offline analysis. To account for dye washout, absorbance was calculated from a reflectance scan at 500–600 nm taken after each time-based fluorescence scan. At the end of the experiment, the heart was tetanized with a bolus of 20 mM $CaCl_2$ with 10 μM cyclopiazonic acid (Sigma Chemical, St. Louis, MO) to determine the maximum fluorescence (F_{max}).

Quantification of the relative amount of rhod-2 in the heart was done by taking the ratio of reflectance at 524 nm (R_{524}, rhod-2 sensitive) to 589 nm (R_{589}, rhod-2 insensitive). Rhod-2 absorbance (A) was calculated according to the following formula (9, 10):

$$A = \log\left[\frac{\left(\frac{R_{524}}{R_{589}}\right)_0}{\left(\frac{R_{524}}{R_{589}}\right)_{rhod2}}\right] \quad (1)$$

where subscripts "0" and "rhod2" indicate the reflectance ratio before and after dye loading, respectively. Intracellular free calcium was calculated using the following formula:

$$[Ca^{2+}]_i = \frac{\left[\frac{K_d(F_t - F_0)}{A_t}\right]}{\left(\frac{F_{max} - F_0}{A_{max}}\right) - \left(\frac{F_t - F_0}{A_t}\right)} \quad (2)$$

where K_d is the dissociation constant for rhod-2 and calcium (710 nM), F_t and A_t are fluorescence and dye absorbance at time t, F_0 is the fluorescence before dye loading, and F_{max} and A_{max} are maximal fluorescence obtained from the tetanized heart and dye absorbance just before tetanizing the heart, respectively.

Frank-Starling protocol. A reference LV volume (typically 16–18 μl) was set by adjusting the balloon volume to yield a LV end-diastolic pressure of ~5 mmHg. Pressures and fluorescence data were continuously recorded over a 2-min period. The first 20 s corresponded to data at the reference volume, followed by a period wherein LV volume was increased in 2-μl increments to the point when developed pressure had reached its maximum value (Fig. 1). Thereafter, LV volume was held constant at this maximal value (V_{max}), and data were recorded at 5 and 10 min.

Mechanical restitution protocol. All measurements were obtained in this protocol with LV volume set at V_{max} (identified in the Frank-Starling protocol). Pressure and fluorescence data were recorded for steady-state contractions at the control pacing interval of 240 ms (i.e., control pulse interval, CPI) and for a test contraction with a single-beat perturbation of the pacing interval (i.e., test pulse interval, TPI). To achieve a range of pressure and calcium pairs, data were collected at four values of TPI (200, 400, 600, and 800 ms) and with the test contraction deployed in three ways: after a steady-state contraction (Fig. 2*A*), after one extra systole at 100 ms (Fig. 2*B*), and after two extra systoles at 100 and 200 ms (Fig. 2*C*). Each experi-

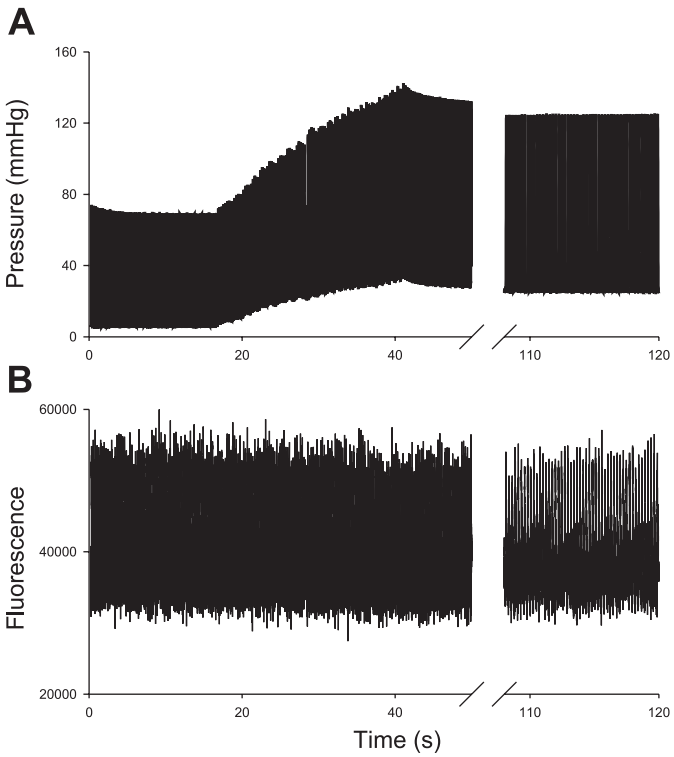

Fig. 1. Typical 2-min recording of (A) left ventricular (LV) pressure and (B) fluorescence data before, during, and after increase in LV volume. LV pressure increased with increments in LV volume; however, there was little change in fluorescence, indicating unaltered intracellular free calcium transient. There were no changes in pressure or fluorescence when LV volume was held constant at the highest value for 80 s.

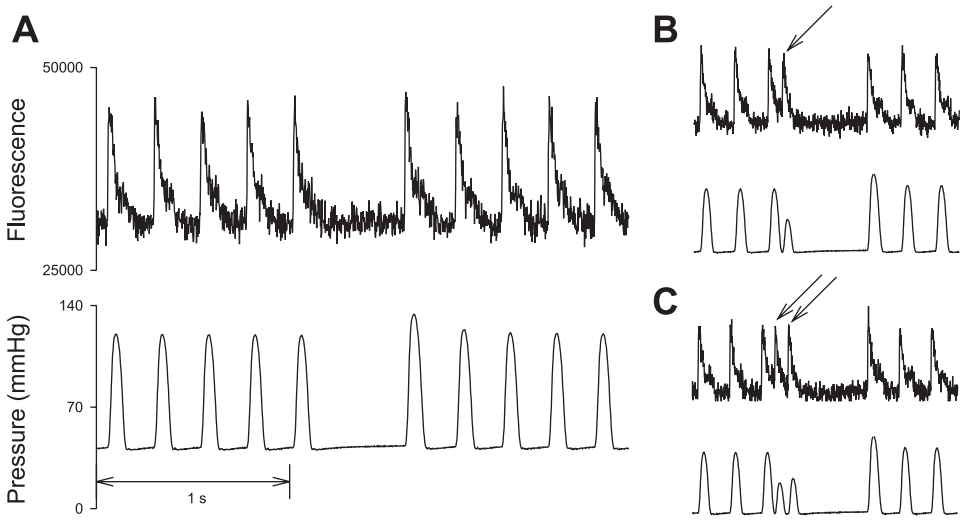

Fig. 2. Examples of fluorescence and left ventricular (LV) pressure data obtained during mechanical restitution protocols. *A*, *B*, and *C* correspond to *protocol 1* (test pulse interval = 600 ms, no extra systole), *protocol 2* (test pulse interval = 600 ms, 1 extra-systole indicated by arrow), and *protocol 3* (test pulse interval = 600 ms, 2 extra-stimuli indicated by arrows), respectively. Following a prolonged test pulse interval there was potentiation of both LV pressure and systolic calcium with respect to the steady-state contractions.

mental condition (i.e., a combination of TPI value and mode of deployment) was repeated four to five times.

Data analysis. Individual cardiac cycles were first identified by using the spike in the pacer signal. Signal averaging over the cardiac cycle was then performed to reduce high-frequency random noise, especially in the calcium fluorescence signal. For the Frank-Starling protocol, pressure and fluorescence data from five to seven steady-state contractions at a given LV volume were averaged to yield a representative cycle. For the mechanical restitution protocol, up to five of the repeated measurements of each experimental condition were averaged to yield one representative cycle each for control and test contractions. LV pressure and calcium waveforms were characterized by several amplitude and rate indexes. Amplitude indexes included diastolic pressure (P_{dia}) and calcium ($[Ca]_{i\text{-}dia}$), peak systolic pressure (P_{sys}), and calcium ($[Ca]_{i\text{-}sys}$), and developed pressure ($P_{dev} = P_{sys} - P_{dia}$) and calcium ($[Ca]_{i\text{-}dev} = [Ca]_{i\text{-}sys} - [Ca]_{i\text{-}dia}$). Rate indexes included maximal rate of rise (dP/dt_{max}, $d[Ca]_i/dt_{max}$), maximal rate of fall (dP/dt_{min}, $d[Ca]_i/dt_{min}$), rise time ($T_{rise\text{-}P}$, $T_{rise\text{-}Ca}$), and relaxation time ($T_{relax\text{-}P}$, $T_{relax\text{-}Ca}$). T_{relax} was defined as the time taken for developed pressure (or calcium) to decay from 75% to 25% of its maximum value. Similarly, T_{rise} was defined as the time taken for pressure (or calcium) to rise from 25% to 75% of its maximum value. Finally, the calcium area ($[Ca]_{i\text{-}area}$) was calculated as the area under the calcium transient. Calculations of T_{relax}, T_{rise}, and $[Ca]_{i\text{-}area}$ were performed after the diastolic value of pressure (or calcium) waveform was subtracted, such that each waveform rose from and declined to zero.

Data are expressed as means ± SE. Repeated measures analysis of variance and Tukey's HSD post hoc test were used to evaluate the effects of acute changes in LV volume loading on pressure and calcium variables, the effects of time on these variables, and the effects of stimulus interval in the mechanical restitution data. To relate percentage changes from baseline values in two variables, linear regression analysis was performed with the constraint of zero intercept.

RESULTS

Frank-Starling protocol. An example of the Frank-Starling protocol data from one heart is illustrated in Fig. 3*A*, showing marked changes in pressure with little change in the calcium transient. In eight hearts, P_{sys} increased from 62.3 ± 5.5 to 120.2 ± 9.0 mmHg when LV volume was raised from 16.5 ± 0.3 to 30.6 ± 0.3 μl. As illustrated in Fig. 4, P_{dia}, P_{dev} (Fig. 4*A*), $(dP/dt)_{max}$, and $(dP/dt)_{min}$ significantly increased (all $P <$ 0.05) and $T_{relax\text{-}P}$ or $T_{rise\text{-}P}$ (Fig. 4*B*) was unchanged with increments in LV volume. Thus changes in LV volume simply scaled the developed pressure waveform without any significant alterations in its morphology. In contrast, there were no significant changes in any of the indexes calculated from calcium transients (Fig. 4, *C* and *D*).

At 10 min after the increase in LV volume to V_{max}, there was a small, but significant, decrease in P_{dev} and P_{dia} (6% and 8%, respectively, both $P < 0.05$) (Fig. 5*A*). None of the $[Ca]_i$ indexes (e.g., $[Ca]_{i\text{-}sys}$, $[Ca]_{i\text{-}dia}$, and $T_{relax\text{-}Ca}$) changed significantly over this time (Fig. 5, *B* and *C*).

Mechanical restitution protocol. An example of the mechanical restitution protocol data from one heart is illustrated in Fig. 3*B*, showing marked changes in pressure due to TPI alterations at a fixed LV volume. As summarized in Table 1, an increase in TPI increased P_{sys}, P_{dev} , $(dP/dt)_{max}$, $(dP/dt)_{min}$, and $T_{relax\text{-}P}$. For example, with respect to the control beat values, P_{sys}, P_{dev}, $(dP/dt)_{max}$, $(dP/dt)_{min}$, and $T_{relax\text{-}P}$ increased at TPI = 600 ms by 23.8 ± 1.2% ($P < 0.01$), 31.3 ± 1.2% ($P < 0.01$), 28.0 ± 1.4% ($P < 0.01$), 7.8 ± 1.1% ($P < 0.01$), and 21.2 ± 1.9% ($P < 0.01$), respectively.

Unlike the results from the Frank-Starling protocol, there were significant changes in $[Ca]_i$ dynamics, along with small, but significant, changes in $[Ca]_i$ peak magnitude. As illustrated in Table 1, an increase in TPI increased $[Ca]_{i\text{-}sys}$, $[Ca]_{i\text{-}dev}$, $T_{relax\text{-}Ca}$, and $[Ca]_{i\text{-}area}$. For example, with respect to the control beat values, $[Ca]_{i\text{-}sys}$, $[Ca]_{i\text{-}dev}$, $T_{relax\text{-}Ca}$, and $[Ca]_{i\text{-}area}$ increased at TPI = 600 ms by 7.4 ± 1.4% ($P < 0.01$), 10.6 ± 1.8% ($P <$ 0.01), 30.0 ± 5.5% ($P < 0.01$), and 29.2 ± 2.2% ($P < 0.01$), respectively. TPI did not affect $T_{rise\text{-}Ca}$; it remained very fast under all conditions ($T_{rise\text{-}Ca}$ = 8 ± 1 ms). Given that $[Ca]_{i\text{-}area}$ increased much more than $[Ca]_{i\text{-}sys}$, the major contributor to the area increase was the prolonged time of calcium transient decay (i.e., increased $T_{relax\text{-}Ca}$). These results indicate that the increase in developed pressure with increasing TPI is associated with a small, but significant, increase in peak systolic calcium and marked prolongation of both pressure and calcium relaxation.

As mentioned earlier, the three TPI deployment modes (Fig. 2) were used merely to create a wide variety of pressure and calcium pairs. Clearly, changes in pressure at a given TPI are

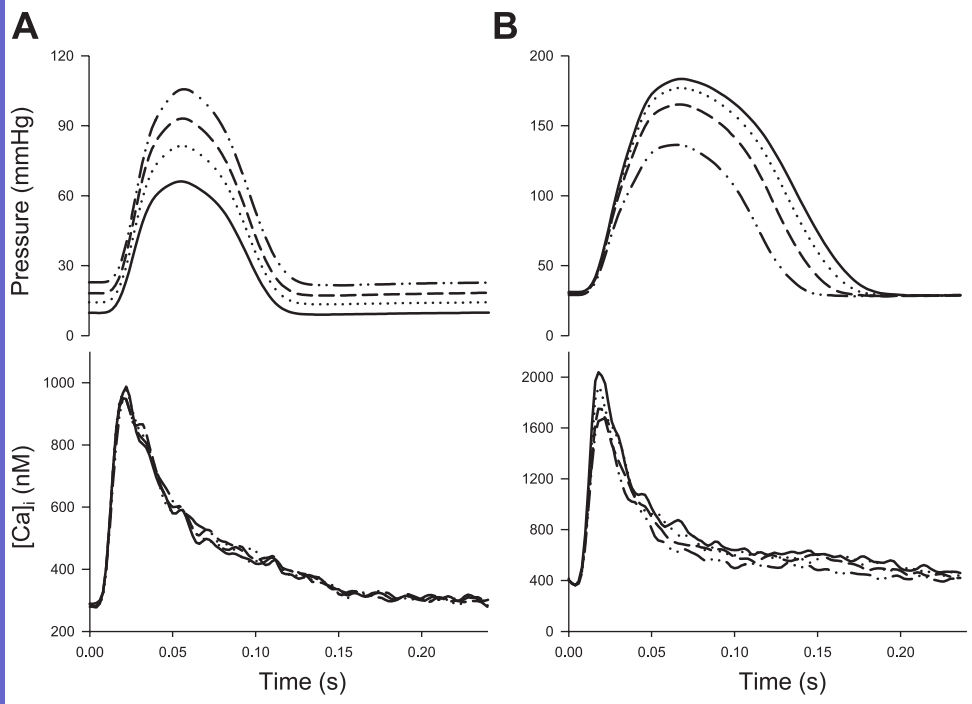

Fig. 3. Examples of averaged LV pressure and intracellular free calcium transient ($[Ca]_i$) data during a cardiac cycle from the Frank-Starling (*A*) and mechanical restitution (*B*) protocols. *A*: as LV volume was increased, there were significant changes in the LV pressure without any accompanying changes in $[Ca]_i$. *B*: during single-beat alterations in pacing interval at a fixed volume, both LV pressure and $[Ca]_i$ changed.

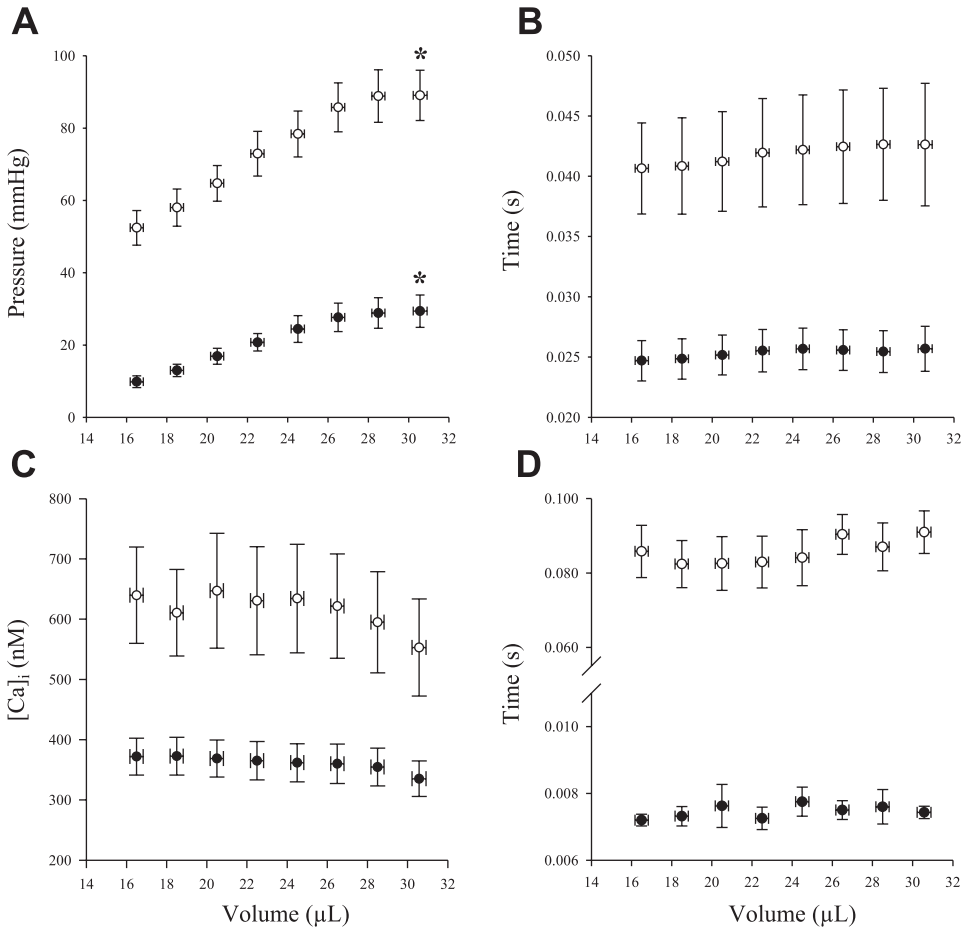

Fig. 4. Effects of altered LV volume on indexes of pressure (*A* and *B*) and $[Ca]_i$ (*C* and *D*). With increments in LV volume, LV end-diastolic pressure (●) and developed pressure (○) significantly increased (*A*), with no changes in either pressure rise time (●) or pressure relaxation time (○) (*B*). In contrast, neither the magnitude (*C*; ●: diastolic $[Ca]_i$, ○: developed $[Ca]_i$) nor the morphology (*D*; ●: $[Ca]_i$ rise time, ○: $[Ca]_i$ relaxation time) were altered with increments in LV volume. Data are means ± SE. $^*P < 0.05$ for ANOVA with repeated measures.

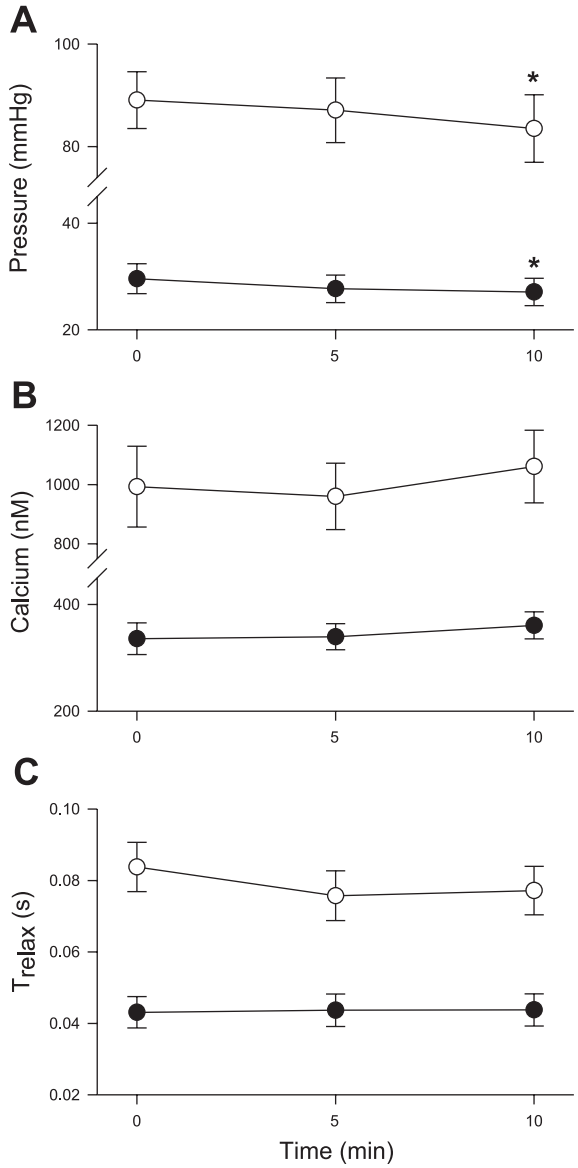

Fig. 5. Effects of sustained volume over a 10-min period. *A*: LV developed pressure (○) and LV end-diastolic pressure (●). *B*: systolic $[Ca]_i$ (○) and diastolic $[Ca]_i$ (●). *C*: $[Ca]_i$ relaxation time (●) and LV pressure relaxation time (●). There were small, but significant, decrements in LV developed and end-diastolic pressures over the 10-min period, though there were no changes in any of the $[Ca]_i$ indexes or LV pressure relaxation time. Data are means ± SE. $*P < 0.05$ ANOVA with repeated measures.

not expected to be the same for the three TPI deployment modes. This is the reason for the relatively large standard errors in Table 1. Instead of pooling data by TPI, we plotted percentage changes in rise and relaxation times against the corresponding percentage change in P_{dev} and $[Ca]_{i\text{-}dev}$ for all experiments and all conditions within an experiment (i.e., 4 TPI settings and 3 TPI deployment modes). This was done to assess whether changes in waveform morphology were related to the changes in waveform magnitude. All percentage changes were computed with respect to the control beat values (i.e., steady-state contractions at pacing interval of 240 ms).

As P_{dev} increased, there was no change in $T_{rise\text{-}P}$ (Fig. 6*A*) and $T_{relax\text{-}P}$ increased (Fig. 6*B*). Similar correlations existed for the calcium data as well (Fig. 6, *C* and *D*), i.e., invariant $T_{rise\text{-}Ca}$ (Fig. 6*C*) and increasing $T_{relax\text{-}Ca}$ (Fig. 6*D*) with increments in $[Ca]_{i\text{-}dev}$. There was greater variability in the calcium data, which is attributable to lower signal-to-noise ratio associated with fluorescence-based calcium measurements.

The percentage change in $T_{relax\text{-}P}$ ($\Delta T_{relax\text{-}P}$) was positively correlated to the percentage change in $T_{relax\text{-}Ca}$ ($\Delta T_{relax\text{-}Ca}$) (Fig. 7, $R^2 = 0.53$; $P < 0.001$), indicating that the slower pressure relaxation can be explained in terms of the slower calcium relaxation. To examine how percentage changes in P_{dev} (ΔP_{dev}) are related to changes in various indexes of $[Ca]_i$, ΔP_{dev} is plotted against percentage changes in three selected indexes of $[Ca]_i$ (Fig. 8): $\Delta[Ca]_{i\text{-}sys}$, $\Delta T_{relax\text{-}Ca}$, and $\Delta[Ca]_{i\text{-}area}$. Whereas each of the three relationships had a significant positive correlation, the slope of ΔP_{dev}-$\Delta[Ca]_{i\text{-}sys}$ relationship (2.30, Fig. 8*A*) was significantly greater than that of ΔP_{dev}-$\Delta T_{relax\text{-}Ca}$ relationship (0.96, Fig. 8*B*) or ΔP_{dev}-$\Delta[Ca]_{i\text{-}area}$ relationship (0.93, Fig. 8*C*). Thus TPI-induced changes in developed pressure are associated with small changes in peak systolic calcium and large changes in $[Ca]_{i\text{-}area}$ (almost 1:1) that are mostly due to the marked prolongation of calcium relaxation. Furthermore, slower pressure relaxation is mostly attributable to this prolongation of calcium relaxation.

DISCUSSION

Our data demonstrate unique features of the calcium-pressure relationship in the intact mouse heart. During the length-dependent increase in contraction, LV developed pressure increased immediately, but the secondary rise seen in larger mammals was absent. None of the indexes of pressure waveform shape or the calcium transient (magnitude and/or waveform shape including relaxation) were altered significantly. Single-beat changes in stimulus interval at a fixed ventricular volume also produced marked changes in developed pressure. However, an increase in pressure in this case was associated with marked increases in pressure and calcium relaxation times and a small, but significant, rise in the peak of the calcium transient. Finally, pressure relaxation was load independent and primarily governed by calcium relaxation (removal).

Pressure modulation via changes in muscle length. Studies (1) in isolated muscles from rats and cats have shown that increases in muscle length produce an immediate increase in force, although no change in the peak of the calcium transient, followed by slow increases in calcium and force that are similar in both magnitude and time course. Todaka et al. (28) have observed a similar pattern of response in the canine, blood-perfused isolated heart; following the immediate increase in pressure resulting from myocardial stretch, pressure and intracellular free calcium rose slowly for 3 min. In contrast to these studies, Reyes et al. (23), who studied in vivo hemodynamics in the mouse, showed that there was no secondary (late) increase in contractility (pressure) following an increase in LV end-diastolic volume brought about by aortic constriction. Our data are consistent with these observations and add to the study of Reyes et al. by showing that the constant pressure is accompanied by an absence of changes in the intracellular free calcium transient over a 10-min period.

The explanation for the difference between the mouse and other mammalian hearts could be based on the aforementioned limited dependence on sarcolemmal calcium transport. Alvarez

Table 1. *Summary of data from the mechanical restitution protocol*

	Interval, ms			
	200	240 (control)	400	600
Pressure data				
P_{sys}, mmHg	102.9±4.3	106.5±4.0	123.9±4.7†	133.3±5.1†
P_{dia}, mmHg	28.5±1.7	28.4±1.7	29.2±1.7†	29.6±1.9†
P_{dev}, mmHg	74.4±4.2	78.1±4.0	94.7±4.9†	103.8±5.5†
dP/dt_{max}, mmHg/s	3,028±138	3,108±123	3,657±148†	3,960±155†
dP/dt_{min}, mmHg/s	−1,916±107	−1,982±102	−2,148±105†	−2,159±105†
$T_{rise\text{-}P}$, ms	26.2±1.0†	26.7±1.0	27.1±1.1	27.2±1.2
$T_{relax\text{-}P}$, ms	43.1±2.9	43.8±3.0	49.0±3.6†	53.6±4.4†
Calcium data				
$[Ca]_{i\text{-}sys}$, nM	948±59*	990±63	1,009±63	1,094±72†
$[Ca]_{i\text{-}dia}$, nM	365±14*	381±15	375±15	394±15
$[Ca]_{i\text{-}dev}$, nM	582±54	610±57	633±58	700±66†
$[Ca]_{i\text{-}area}$, nM·s	24.8±2.3	25.3±2.1	29.8±2.7†	34.0±2.9†
$T_{rise\text{-}Ca}$, ms	8.3±0.3	8.4±0.4	8.2±0.4	8.3±0.4
$T_{relax\text{-}Ca}$, ms	79.9±4.2	82.5±3.6	91.6±5.2	105.9±5.1†

Values are means ± SE. P_{sys}, left ventricular (LV) peak systolic pressure; P_{dia}, LV diastolic pressure; P_{dev}, LV developed pressure; dP/dt_{max}, maximal rate of rise of LV pressure; dP/dt_{min}, maximal rate of fall of LV pressure; $T_{rise\text{-}P}$, LV pressure rise time; $T_{relax\text{-}P}$, LV pressure fall time; $[Ca]_{i\text{-}sys}$, peak systolic intracellular free calcium concentration; $[Ca]_{i\text{-}dia}$, diastolic intracellular free calcium; $[Ca]_{i\text{-}dev}$, developed intracellular free calcium; $[Ca]_{i\text{-}area}$, area under the intracellular free calcium transient; $T_{rise\text{-}Ca}$, calcium rise time; $T_{relax\text{-}Ca}$, calcium fall time. (Note: limited data were available at test pulse interval (TPI) = 800 ms because there was often a spontaneous contraction before the desired stimulation interval. Therefore, data for this TPI are not included in this table; though they are included Figs. 6–8.) *$P < 0.05$, †$P < 0.01$, vs. 240-ms pacing interval, Tukey/Kramer post hoc test if repeated measures ANOVA showed a significant difference.

et al. (2) demonstrated that the secondary increase in force and calcium in rat ventricular trabeculae is related to activation of the Na^+/H^+ exchanger, which increases intracellular sodium and leads to an increase in intracellular calcium. However, because sarcolemmal calcium transport in the mouse plays such a small role in excitation-contraction coupling (4, 18), this sarcolemmal mechanism of the secondary increase in intracellular calcium may not be operative in the mouse, leading to a lack in augmentation of the calcium transient found in other species. Additionally, a tertiary decrease has been observed following the secondary rise that returned calcium and pressure levels to the presecondary rise levels (28). The mechanism for

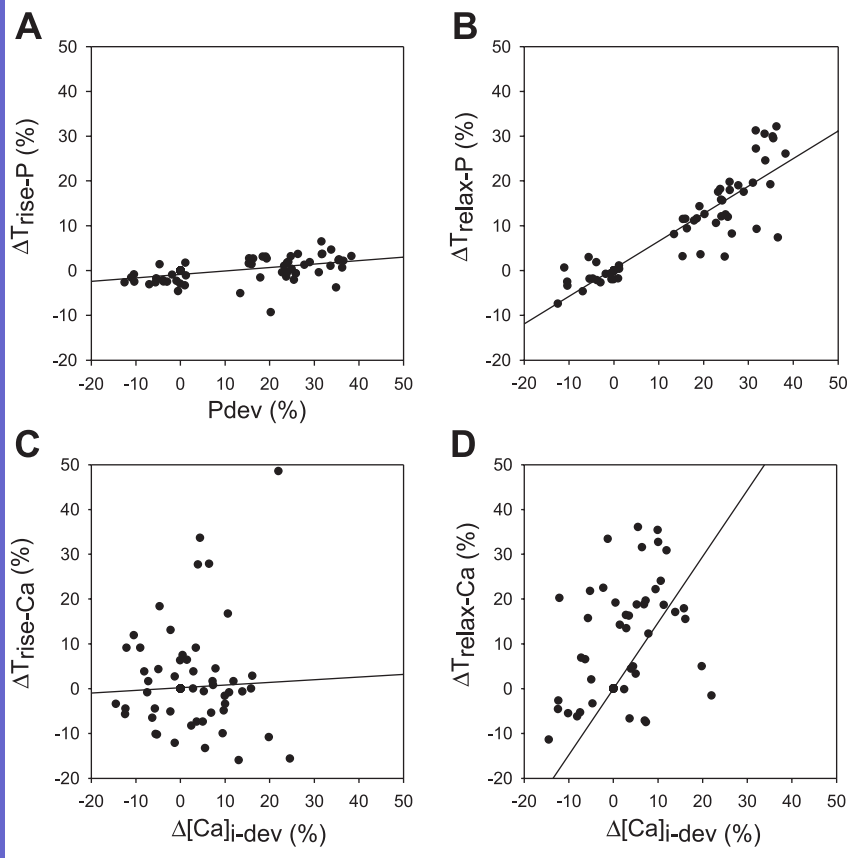

Fig. 6. Analysis of mechanical restitution data from all experiments to examine morphological changes in LV pressure and $[Ca]_i$ signals individually. *A* and *B*: Percentage changes in LV pressure rise ($\Delta T_{rise\text{-}P}$) and relaxation ($\Delta T_{relax\text{-}P}$) times with respect to the control beat values are plotted as a function of the percentage change in LV developed pressure (ΔP_{dev}). $\Delta T_{rise\text{-}P}$ was independent of ΔP_{dev} (*A*; slope = 0.05, $P < 0.001$). In contrast, $\Delta T_{relax\text{-}P}$ increased with increasing ΔP_{dev} (*B*; slope = 0.63, $P < 0.001$), indicating relative slowing of pressure relaxation. *C* and *D*: Percentage changes in $[Ca]_i$ rise ($\Delta T_{rise\text{-}Ca}$) and relaxation ($\Delta T_{relax\text{-}Ca}$) times with respect to the control beat values are plotted as a function the percentage change in developed $[Ca]_I$ ($\Delta[Ca]_{i\text{-}dev}$). $\Delta T_{rise\text{-}Ca}$ was independent of $\Delta[Ca]_{i\text{-}dev}$ (*C*; slope = 0.07, $P = 0.73$). In contrast, $\Delta T_{relax\text{-}Ca}$ increased with increasing $\Delta[Ca]_{i\text{-}dev}$ (*D*; slope = 1.48, $P < 0.001$), indicating relative slowing of calcium relaxation.

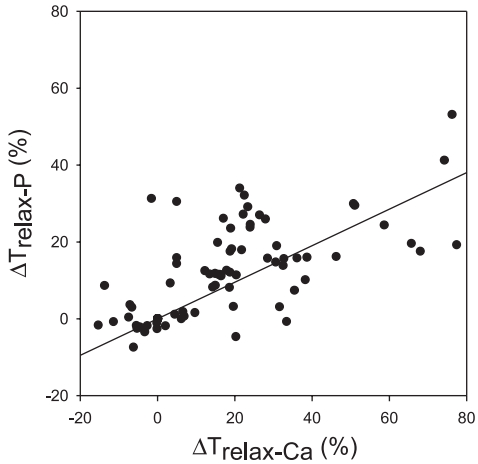

Fig. 7. Analysis of mechanical restitution data from all experiments to examine the relationship between morphological changes in LV pressure and $[Ca]_i$ signals. The percentage change in LV pressure relaxation ($\Delta T_{relax\text{-}P}$) was positively correlated with the percentage change in $[\Delta Ca]_i$ relaxation ($T_{relax\text{-}Ca}$): slope = 0.48, R^2 = 0.53, $P < 0.001$.

this tertiary drop is not understood, but if the time courses of the late-phase rise and tertiary drop are comparable in the mouse, these two phenomena can offset each other, resulting in no late changes in calcium.

Given that our perfusion medium (supplemented Media 199, see METHODS) has lower oxygen-carrying capacity than blood, one needs to consider potentially confounding effects of hypoxia, especially at high LV volumes. We do not believe that hypoxia was a significant confounder in our experiments for the following two reasons. First, our group average P_{dev} value (89 mmHg at LV volume = 30 μl) is comparable to that reported by Eberli et al. (11) for blood-perfused mouse hearts [$P_{dev} \approx 85$ mmHg at LV volume = 30 μl, inferred from Fig. 2 of Eberli et al. (11)]. Thus the oxygenation status of our perfusate does not seem to be a limiting factor for LV contraction. Second, sustained hypoxia is known to cause an increase in P_{dia} and a decrease P_{dev} at a fixed LV volume. Although we did see a small decrease in P_{dev} at a fixed LV volume and over a 10-min period (Fig. 5, 89 to 84 mmHg), we did not observe any rise in the P_{dia}. In fact, there was a slight decrease in P_{dia} over the 10-min period of sustained high LV volume (30 to 27 mmHg, Fig. 5). Thus there is no evidence of hypoxia in our preparation.

Pressure modulation via transient changes in stimulation interval. Wier and Yue (29) have described the relationship between calcium and force during transient alterations of stimulation interval in isolated ferret papillary muscles. They demonstrated a linear relationship between force and peak intracellular free calcium, with an increase in peak intracellular free calcium of 1 μM producing a large increase in force of 0.03 N/mm^2. Moreover, they showed that the percentage increase in peak force was nearly equal to the percentage increase in peak calcium, indicating a one-to-one relative increase over a wide range (several times the baseline values). Whereas we also saw large increases in peak pressure (up to 50%), the maximum increase in peak calcium was only 20%. In other words, an increase in systolic calcium was associated with an increase in developed pressure of much greater magnitude (Fig. 8*A*). This observation of high calcium-pressure "gain" is consistent with significantly greater cooperativity (Hill coefficient = 9.9) reported by Gao et al. (12) in constantly activated mouse myocardium compared with that of larger mammals. They also reported that that the positive force-frequency relationship (FFR) in mouse myocardium was accompanied by relatively small changes in intracellular free calcium for stimulation frequencies above 2 Hz, a phenomenon

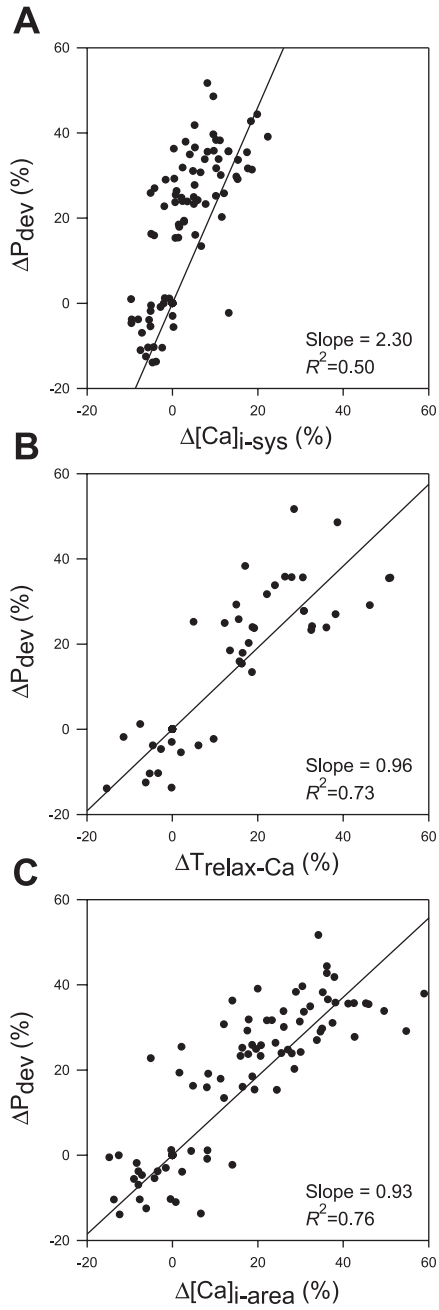

Fig. 8. Analysis of mechanical restitution data from all experiments to examine how the percentage change in LV developed pressure (ΔP_{dev}) is related to percentage changes in various indexes of $[Ca]_i$. *A*: $\Delta P_{dev} - \Delta[Ca]_{i\text{-}sys}$ (changes in peak systolic $[Ca]_i$). *B*: $\Delta P_{dev} - \Delta T_{relax\text{-}Ca}$ (changes in $[Ca]_i$ relaxation time). *C*: $\Delta P_{dev} - \Delta[Ca]_{i\text{-}area}$ (change in area under the calcium transient). While ΔP_{dev} was positively correlated with all three $\Delta[Ca]_i$ indexes, the slope of $\Delta P_{dev} - \Delta[Ca]_{i\text{-}sys}$ relationship was significantly greater than the slopes of the other two relationships.

they referred to as "frequency-dependent sensitization of myofilaments."

Our results show that P_{dev} and $[Ca]_{i\text{-}area}$ in the mouse increase almost one-to-one (Fig. 8*C*). The increased $[Ca]_{i\text{-}area}$ is only slightly modulated by the increased peak; instead, a slowed decay of the calcium transient is the major contributor (Fig. 8*B*). This observation supports the premise that the temporal pattern of the calcium transient, not just the peak, significantly influences developed pressure in the mouse heart. Slower decay of the calcium transient may be due to one or more of the following: *1*) the rate of calcium uptake is near maximal under baseline conditions so that the calcium transient amplitude would be higher and calcium decay would be slower when more calcium is released (as would be expected for a contraction with increased pacing interval); *2*) sarcoplasmic reticulum calcium uptake is reduced; and/or *3*) there is increased troponin C calcium binding (14) due to increased myofilament calcium sensitivity. All of these postulated mechanisms of delayed decay of the calcium transient are likely to increase pressure because there is prolonged calcium binding to troponin C and consequent prolonged actomyosin cross-bridge interactions.

Developed pressure and calcium. Our data indicate that significant changes in LV peak developed pressure can occur in the mouse heart with little or no change in peak of the calcium transient. This behavior in the mouse heart is quite different from what has been reported for higher mammals (1, 21, 28). This lack of peak calcium variation may be a result of calcium cycling functioning at near maximal capacity at baseline in the mouse heart. We recognize that β-adrenergic agonists can significantly increase peak intracellular free calcium in the isolated mouse heart (20). However, given its high baseline heart rate and limited ability to increase heart rate via sympathetic activation, indicating high basal sympathetic tone (13), this physiological mechanism may not be available to the mouse in vivo. Our observation of high calcium-pressure gain and increased cooperativity reported by others (12) can be considered as compensatory responses to offset the limited ability for modulating calcium transient amplitude in the mouse heart.

Determinants of pressure relaxation. Increased load prolongs force relaxation in mammalian ventricular muscle preparations (5). Specifically, an increase in developed stress, brought about by an increase in muscle stretch, is associated with prolonged relaxation in isolated, isovolumically contracting ferret hearts (27) and in isosarcometrically contracting isolated rat trabeculae (7). Two potential mechanisms have been postulated for this prolongation of pressure (force) relaxation: *1*) changes in calcium transient, particularly its prolonged relaxation, and *2*) existence of cooperative feedback mechanisms, including cross-bridge-myofilamental activation cooperativity and cross-bridge-to-cross-bridge cooperativity (7, 15, 27). In contrast to these observations from other mammalian species, we did not observe any load-dependent changes in calcium transients or pressure waveform morphology in the Frank-Starling protocol. In agreement with these findings, Reyes et al. (23) have shown that afterload increases in the in vivo mouse model do not affect active relaxation.

We did observe prolonged pressure relaxation with increasing developed pressure in the mechanical restitution protocol (Fig. 6*B*). However, this prolongation can be attributed to slower decay of the calcium transient (Fig. 7). This observation, together with results from the Frank-Starling protocol, indicates that pressure (force) relaxation in the mouse is primarily governed by calcium removal; cross-bridge-mediated control of relaxation, typically seen other mammalian species, is either absent (minimal) or operating near saturation under the baseline conditions. Given the increased cooperativity of constantly activated mouse myocardium (Hill coefficient = 9.9) (12), the latter possibility is more likely. Teleologically, this load independence of pressure relaxation may help maintain cardiac function in the setting of high heart rates.

Model-based analysis. A model-based analysis was performed to obtain additional insights into the dynamics of pressure-calcium relationships. Specifically, a four-state model (3, 6, 25, 26) was used to predict the pressure waveform for a given calcium transient and model parameters. Details regarding this model and associated analysis steps are presented in the APPENDIX.

In the mechanical restitution protocol, there were changes in the magnitude and shape of calcium and pressure waveforms (Fig. 9*A*). Given the similarity in directional changes in the indexes of calcium and pressure transients, we hypothesized that the changes in the pressure waveform were due entirely to changes in the calcium transient. Specifically, with respect to the control condition, $[Ca]_{i\text{-}dev}$, $T_{relax\text{-}Ca}$, P_{dev}, and $T_{relax\text{-}P}$ increased at TPI of 600 ms by 13%, 28%, 39%, and 22%, respectively. When the magnitude and relaxation of the model-input calcium transient were altered to match experimentally observed changes during altered stimulation interval, the model output reproduced experimentally observed alterations in the developed pressure waveform (Fig. 9*B*) without any perturbations in the model parameters. These results support our hypothesis and indicate that there is no need to invoke any changes in the dynamic processes that link calcium to pressure (i.e., model parameters) to reconcile observed calcium-pressure data from the mechanical restitution protocol. However, one cannot rule out the possibility of multiple, mutually offsetting changes in model parameters on the basis of this analysis.

In the Frank-Starling protocol there were no changes in the calcium transient, but the developed pressure increased significantly (101%), whereas $T_{rise\text{-}P}$ and $T_{relax\text{-}P}$ increased by modest amounts (8% and 5%, respectively) (Fig. 10*A*). From the modeling perspective, if the input to the system (calcium transient) is not changing and the output (pressure transient) is, then the parameters describing the system must be changing. In other words, certain model parameters are volume or stretch dependent. Based on the results of Shimizu et al. (25), the following model parameters were considered to be stretch dependent: *1*) two parameters (K_3 and K_4) corresponding to calcium dissociation from troponin C, *2*) two parameters corresponding to cross-bridge formation (f) and dissolution (g'), and *3*) the gain parameter (α) that converts molar concentration of force generating states to pressure (force).

Effects of changes in stretch-dependent model kinetic parameters (i.e., *categories 1* and *2* listed above) are illustrated in Fig. 10*B*. Data from Shimizu et al. (25) were used to alter these model parameter values. Whereas this perturbation increased developed pressure by an appropriate amount (109%), it also increased $T_{rise\text{-}P}$ and $T_{relax\text{-}P}$ by 14% and 94%, respectively,

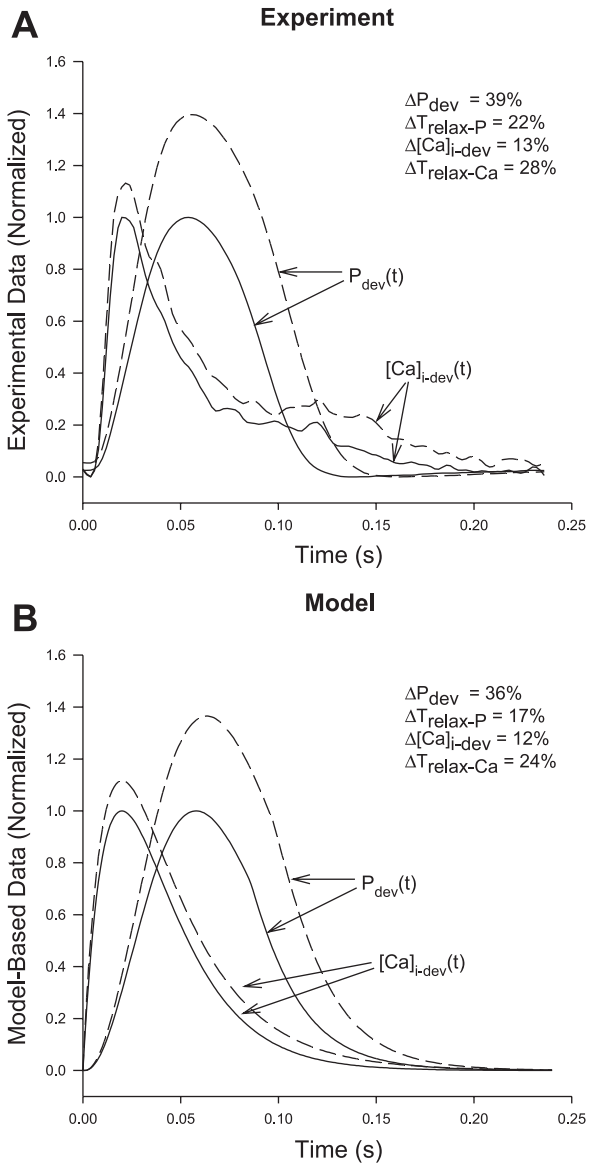

Fig. 9. Comparison of the model-based prediction and experimentally measured data obtained with the mechanical restitution protocol. *A*: experimentally measured LV developed pressure waveform, $P_{dev}(t)$ and developed $[Ca]_i$ waveform, $[Ca]_{i\text{-}dev}(t)$ (solid lines: control pacing interval of 240 ms; dashed lines: test pulse interval of 600 ms). Data are normalized by the peak value of each signal under the control condition. When the pacing interval was transiently increased to 600 ms, both pressure and $[Ca]_i$ changed as indicated. $\Delta[Ca]_{i\text{-}dev}$: change in developed $[Ca]_i$; $\Delta T_{relax\text{-}Ca}$: change in $[Ca]_i$ relaxation time; P_{dev}: change in LV developed pressure; $\Delta T_{relax\text{-}P}$: change in pressure relaxation time. *B*: model-based analysis (solid lines: control pacing interval of 240 ms; dashed lines: test pulse interval of 600 ms). Experimentally measured pressure and calcium data for the control condition were first used to estimate the calcium input function and the four-state model parameters (see APPENDIX). When the calcium input function was altered to match experimentally observed data, the model pressure output reproduced experimentally observed alterations in the developed pressure waveform, without any need to change the four-state model parameters.

which is inconsistent with the experimental observations (especially for the change in $T_{relax\text{-}P}$).

Effects of an increase in the gain parameter (α) are illustrated in Fig. 10*C*. We see a simple amplification of the pressure waveform by 100% with no change in either $T_{rise\text{-}P}$ or

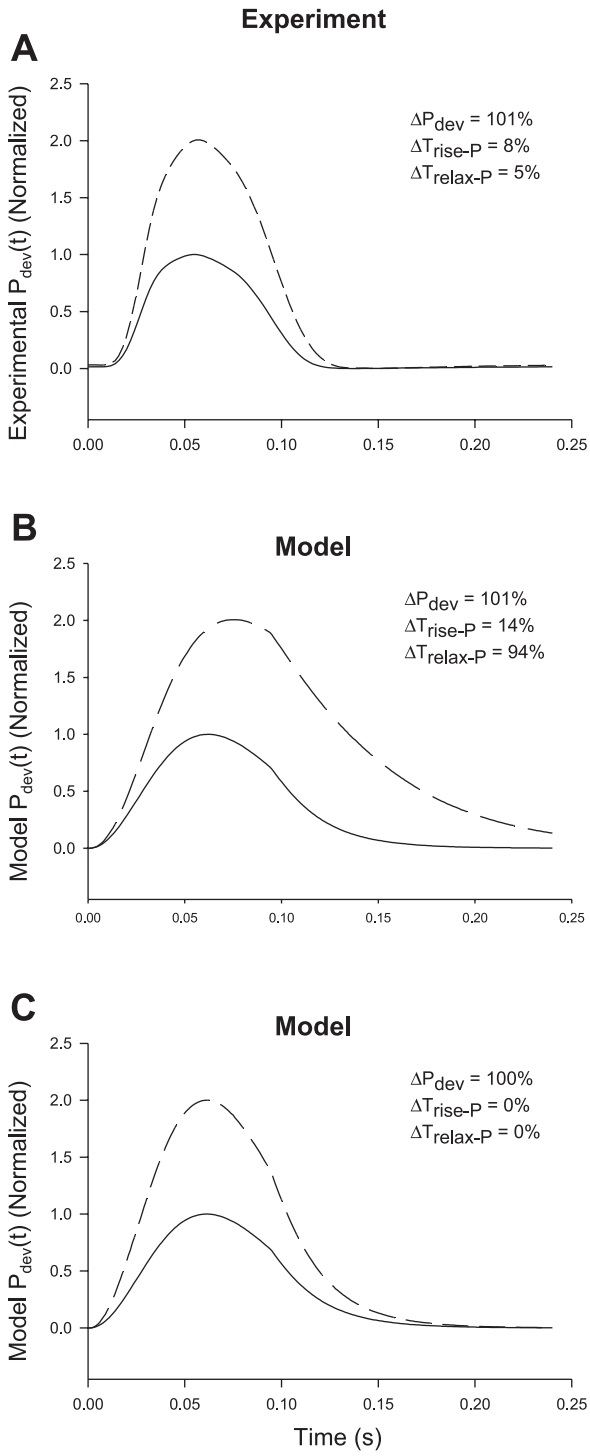

Fig. 10. Comparison of the model-based prediction and experimentally measured data obtained with the Frank-Starling protocol. *A*: experimentally measured LV developed pressure waveform, $P_{dev}(t)$, at two LV volumes: low (solid line) and high (dashed line). Data are normalized by the peak developed pressure (P_{dev}) at low volume. P_{dev} doubled with the increase in LV volume, with little changes in pressure rise ($T_{rise\text{-}P}$) and relaxation ($T_{relax\text{-}P}$) times and $[Ca]_i$ (not shown). *B*, *C*: model-based analysis. Experimentally measured pressure and calcium data for the low volume condition were first used to estimate the calcium input function and the four-state model parameters (see APPENDIX). Model-based prediction of changes in $P_{dev}(t)$ when the stretch-dependent kinetic parameters were altered (*B*) and when the stretch-dependent gain parameter was altered (*C*) (see text).

$T_{relax\text{-}P}$. Clearly, this perturbation satisfactorily captures both the magnitude and temporal features of the pressure response to increased volume. Although the physiological meaning of this gain parameter is not entirely understood, an increase in its value may indicate an increase in force generated per cross-bridge. Unfortunately, if we accept that changes in LV volume (muscle length) only affect this gain parameter, the model fails to reproduce length-dependent changes in the steady-state force-pCa relationship observed in the mouse myocardium (8, 17). We are unable to identify specific mechanisms that can simultaneously reproduce both the length-dependent changes in force-pCa and the disconnect between increased P_{dev} and $T_{relax\text{-}P}$. Further studies are necessary to explain this unique length-dependent behavior in the mouse heart.

In conclusion, the mouse myocardium appears to be unique in that significant changes in peak developed pressure can occur with little or no change in the peak of the calcium transient. In addition, unlike other mammalian species, pressure relaxation is load independent and primarily governed by calcium removal. Thus, although genetically engineered mouse models are commonly used to study cardiac structure-function relationships, caution must be exercised while extrapolating findings from these models to the human setting.

APPENDIX

Glossary

[Ca]	Intracellular concentration of free calcium (μM)
[M]	Intracellular concentration of free myosin (μM)
[TnA]	Intracellular concentration of free troponin-tropomyosin/actin complex (μM)
[Ca·TnA]	Intracellular concentration of calcium-troponin-tropomyosin/actin complex (μM)
[TnA·M]	Intracellular concentration of troponin-tropomyosin/actin-myosin complex (μM)
[Ca·TnA·M]	Intracellular concentration of calcium-troponin-tropomyosin/actin-myosin complex (μM)
K_1	Rate constant for binding of calcium and troponin-tropomyosin/actin complex ($\mu M^{-1}\cdot s^{-1}$)
K_2	Rate constant for dissociation of calcium and troponin-tropomyosin/actin-myosin complex ($\mu M^{-1}\cdot s^{-1}$)
K_3	Rate constant for dissociation of calcium and troponin-tropomyosin/actin complex (s^{-1})
K_4	Rate constant for binding of calcium and troponin-tropomyosin/actin-myosin complex (s^{-1})
f	Rate constant for binding of troponin-tropomyosin/actin complex and myosin in presence of bound calcium ($\mu M^{-1}\cdot s^{-1}$)
g	Rate constant for dissociation of troponin-tropomyosin/actin complex and myosin in presence of bound calcium (s^{-1})
g'	Rate constant for dissociation of troponin-tropomyosin/actin complex and myosin in absence of bound calcium (s^{-1})
α_1	Slope of K_1 cooperativity relation ($\mu M^{-1.5}\cdot s^{-1}$)
β_1	Intercept of K_1 cooperativity relation ($\mu M^{-1}\cdot s^{-1}$)
α_f	Slope of f cooperativity relation ($\mu M^{-3}\cdot s^{-1}$)
β_f	Intercept of f cooperativity relation ($\mu M^{-1}\cdot s^{-1}$)
α	Gain parameter ($N\cdot\mu M^{-1}$)
A	Intracellular free calcium transient model gain parameter (μM)
B	Intracellular free calcium transient model time constant 1 (s^{-1})
C	Intracellular free calcium transient model time constant 2 (s^{-1})

The schematic of the four-state model is presented in Fig. A1. This model is governed by five differential equations and two algebraic equations that describe cooperativity (3, 6, 25, 26):

$$\frac{d[TnA]}{dt} = -K_1[Ca][TnA] + K_3[Ca\cdot TnA] + g'[TnA\cdot M] \quad (A1)$$

$$\frac{d[M]}{dt} = g'[TnA\cdot M] - f[Ca\cdot TnA][M] + g[Ca\cdot TnA\cdot M] \quad (A2)$$

$$\frac{d[Ca\cdot TnA]}{dt} = K_1[Ca][TnA] - K_3[Ca\cdot TnA] - f[Ca\cdot TnA][M] + g[Ca\cdot TnA\cdot M] \quad (A3)$$

$$\frac{d[Ca\cdot TnA\cdot M]}{dt} = f[Ca\cdot TnA][M] + K_2[Ca][TnA\cdot M] - (g + K_4)[Ca\cdot TnA\cdot M] \quad (A4)$$

$$\frac{d[TnA\cdot M]}{dt} = K_4[Ca\cdot TnA\cdot M] - g'[TnA\cdot M] - K_2[Ca][TnA\cdot M] \quad (A5)$$

$$K_1(t) = \alpha_1\{[Ca\cdot TnA\cdot M](t) + [TnA\cdot M](t)\}^{0.5} + \beta_1 \quad (A6)$$

$$f(t) = \alpha_f\{[Ca\cdot TnA\cdot M](t) + [TnA\cdot M](t)\}^2 + \beta_f \quad (A7)$$

$$F(t) = \alpha\{[Ca\cdot TnA\cdot M](t) + [TnA\cdot M](t)\} \quad (A8)$$

Initial conditions represent the concentrations (per unit volume of sarcoplasm) at t=0 of each state prior to introduction of free calcium (3, 22):$[TnA]_{(t=0)}$ = 70μM; $[M]_{(t=0)}$ = 20μM; $[Ca\cdot TnA]_{(t=0)}$ = 0μM; $[Ca\cdot TnA\cdot M]_{(t=0)}$ = 0μM; $[TnA\cdot M]_{(t=0)}$ = 0μM.

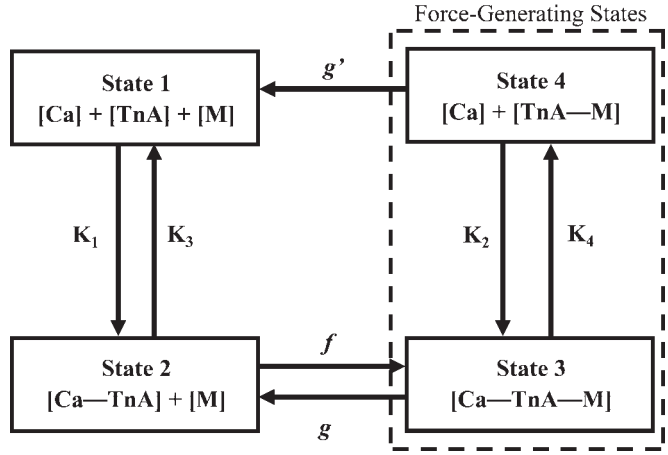

Fig. A1. Block diagram of the four-state model. The status of interaction (+: unbound; −: bound) among calcium ([Ca]), troponin-tropomyosin/actin complex ([TnA]), and myosin ([M]) defines each state. An arrow indicates directional transition between two states; corresponding rate constants are shown next to each arrow (see APPENDIX).

The input calcium transient was represented by the following functional form:

$$[Ca^{2+}]_i = A(1 - e^{-Bt})(e^{-Ct}) \quad (A9)$$

where A, B, and C are parameters that govern amplitude and shape of the calcium transient. For the control condition (i.e., at V_{max} and steady-state pacing interval of 240 ms), $A = 1.839$ μM, $B = 45.89$ s^{-1}, and $C = 30.52$ s^{-1}. These parameters yield $[Ca]_{i\text{-}dev}$, $T_{rise\text{-}Ca}$, and $T_{relax\text{-}Ca}$ of 600 nM, 81 ms, and 10 ms, respectively, which are similar to the experimentally measured values for the control condition (Table 1).

There are 9 model parameters and their nominal values are as follows: α_1 ($\mu M^{-1}\cdot s^{-1}$) = 3.9, β_1 ($\mu M^{-1}\cdot s^{-1}$) = 1.9, α_f ($\mu M^{-1}\cdot s^{-1}$) = 5.2, β_f ($\mu M^{-1}\cdot s^{-1}$) = 90, K_2 ($\mu M^{-1}\cdot s^{-1}$) = 464, K_3 (s^{-1}) = 309, K_4 (s^{-1}) = 12, g (s^{-1}) = 523, g' (s^{-1}) = 709. These values, based on previous observations (24), reproduce the pressure waveform for the control condition.

ACKNOWLEDGMENTS

This study was supported by the National Heart Lung and Blood Institute grants HL-03826 (G. A. MacGowan), HL-68083 (S. G. Schroff), T-32-HL-76124 (J. A. Kirk, predoctoral fellowship), and the McGinnis Chair research funds (S. G. Schroff).

REFERENCES

1. **Allen DG and Kurihara S.** The effects of muscle length on intracellular calcium transients in mammalian cardiac muscle. *J Physiol* 327: 79–94, 1982.
2. **Alvarez BV, Perez NG, Ennis IL, Camilion de Hurtado MC, and Congolani HE.** Mechanisms underlying the increase in force and Ca^{2+} transient that follow stretch of cardiac muscle: A possible explanation of the Anrep effect. *Circ Res* 85: 716–722, 1999.
3. **Baran D, Ogino K, Stennett R, Schnellbacher M, Zwas D, Morgan JP, and Burkhoff D.** Interrelating of ventricular pressure and intracellular calcium in intact hearts. *Am J Physiol* 273: H1509–H1522, 1997.
4. **Bers DM.** Calcium fluxes involved in control of cardiac myocyte contraction. *Circ Res* 87: 275–281, 2000.
5. **Brutsaert DL, DeClerck NM, Goethals MA, and Housmans PR.** Relaxation of ventricular cardiac muscle. *J Physiol* 283: 469–480, 1978.
6. **Burkhoff D.** Explaining load dependence of ventricular contractile properties with a model of excitation-contraction coupling. *J Mol Cell Cardiol* 26: 959–978, 1994.
7. **Campbell KB, Razumova MV, Kirkpatrick RD, and Slinker BK.** Myofilament kinetics in isometric twitch dynamics. *Ann Bio Eng* 29: 384–405, 2001.
8. **Cazorla O, Wu Y, Irving TC, and Granzier H.** Titin-based modulation of calcium sensitivity of active tension in mouse skinned cardiac myocytes. *Circ Res* 88: 1028–1035, 2001.
9. **del Nido PJ, Glynn P, Buenaventura P, Salama G, and Koretsky AP.** Fluorescence measurement of calcium transients in perfused rabbit heart using rhod-2. *Am J Physiol* 274: H728–H741, 1998.
10. **Du C, MacGowan GA, Farkas DL, and Koretsky AP.** Calcium measurements in perfused mouse heart: Quantitating fluorescence and absorbance of rhod-2 by application of photon migration theory. *Biophys J* 80: 549–561, 2001.
11. **Eberli FZ, Sam F, Ngoy S, Apstein CS, and Colucci WS.** Left-ventricular structural and functional remodeling in the mouse after myocardial infarction: Assessment with the isovolumetrically-contracting Langendorff heart. *J Mol Cell Cardiol* 30: 1443–1447, 1998.
12. **Gao WD, Gustavo Perez N, and Marban E.** Calcium cycling and contractile activation in intact mouse cardiac muscle. *J Physiol* 507.1: 175–184, 1998.
13. **Georgakopoulos D and Kass DA.** Minimal force-frequency modulation of inotropy and relaxation of in situ murine heart. *J Physiol* 534.2: 535–545, 2001.
14. **Hajjar RJ, Schmidt U, Helm P, and Gwathmey JK.** Ca^{++} sensitizers impair cardiac relaxation in failing human myocardium. *J Pharmacol Exp Ther* 280: 247–254 1997.
15. **Janssen PML and Hunter WC.** Force, not sarcomere length, correlates with prolongation of isosarcometric contraction. *Am J Physiol* 269: H676–H685, 1995.
16. **Kass DA, Hare JM, and Georgakopoulos D.** Murine cardiac function: A cautionary tail. *Circ Res* 82: 519–22, 1998.
17. **Konhilas JP, Irving TC, Wolska BM, Jweied EE, Martin AF, Solaro RJ, and de Tombe PP.** Troponin I in the murine myocardium: Influence on length-dependent activation and interfilament spacing. *J Physiol* 547.3: 951–961, 2003.
18. **Li L, Chu G, Kranias EG, and Bers DM.** Cardiac myocyte calcium transport in phospholamban knockout mouse: Relaxation and endogenous CaMKII effects. *Am J Physiol* 274: H1335–H1347, 1998.
19. **MacGowan GA, Du C, Glonty V, Suhan JP, Koretsky AP, and Farkas DL.** Rhod-2 based measurements of intracellular calcium in the perfused mouse heart: Cellular and subcellular localization and response to positive inotropy. *J Biomed Opt* 6(1): 23–30, 2001.
20. **MacGowan GA, Du C, and Koretsky AP.** High calcium and dobutamine positive inotropy in the perfused mouse heart: Myofilament calcium responsiveness, energetic economy, and effects of protein kinase C inhibition. *BMC Physiol* 1: 12, 2001.
21. **Maier LS, Barckhausen P, Weisser J, Aleksic I, Baryalei M, and Pieske B.** Ca^{2+} handling in isolated human atrial myocardium. *Am J Physiol Heart Circ Physiol Heart Circ Physiol* 279: H952–H958, 2000.
22. **Peterson JN, Hunter WC, and Berman MR.** Estimated time course of Ca^{2+} bound to troponin C during relaxation in isolated cardiac muscle. *Am J Physiol* 260: H1013–H1024, 1991.
23. **Reyes M, Freeman GL, Escobedo D, Lee S, Steinhelper ME, and Feldman MD.** Enhancement of contractility with sustained afterload in the intact murine heart. *Circ* 107: 2962–2968, 2003.
24. **Rhodes SS, Ropella KM, Audi SH, Camara AKS, Kevin LG, Pagel PS, and Stowe DF.** Cross-bridge kinetics modeled from myoplasmic $[Ca^{2+}]$ and LV pressure at 17°C and after 37°C and 17°C ischemia. *Am J Physiol Heart Circ Physiol Heart Circ Physiol* 284: H1217–H1229, 2003.
25. **Shimizu J, Todaka K, and Burkhoff D.** Load dependence of ventricular performance explained by model of calcium-myofilament interactions. *Am J Physiol Heart Circ Physiol Heart Circ Physiol* 282: H1081–H1091, 2002.
26. **Stennett R, Ogino K, Morgan JP, and Burkhoff D.** Length-dependent activation in intact ferret hearts: Study of steady-state Ca^{2+}-stress-strain interrelations. *Am J Physiol* 270: H1940–H1950, 1996.
27. **Tobias AH, Slinker BK, Kirkpatrick RD, and Campbell KB.** Mechanical determinants of left ventricular relaxation in isovolumically beating hearts. *Am J Physiol* 268: H170–H177, 1995.
28. **Todaka K, Ogino K, Gu A, and Burkhoff D.** Effect of ventricular stretch on contractile strength, calcium transient, and cAMP in intact canine hearts. *Am J Physiol* 274: H990–H1000, 1998.
29. **Wier WG and Yue DT.** Intracellular calcium transients underlying the short-term force-interval relationship in ferret ventricular myocardium. *J Physiol* 376: 507–530, 1986.